Non-enzymatic continuous glucose monitoring system

Sean Moore[1], *Byoung Hee You*[1], *Namwon Kim*[2], *Taehyun Park*[3], *In-Hyouk Song*[1] ✉

[1]*Department of Engineering Technology, Texas State University, San Marcos 78666, USA*
[2]*Ingram School of Engineering, Texas State University, San Marcos 78666, USA*
[3]*School of Mechanical Engineering, Kyungnam University, Changwon-si, Gyeongsangnam-do, Republic of Korea*
✉ *E-mail: in-hyouk.song@txstate.edu*

Published in Micro & Nano Letters; Received on 19th December 2017; Revised on 12th February 2018; Accepted on 19th April 2018

A prominent field of study in biosensor development is the study of electric properties which provide valuable insight into the fluids contents. In this research, a non-enzymatic glucose sensor is fabricated, characterised, and employed. The developed device determines the effects of electrode surface area on sensing efficacy, the effects of glucose concentration on impedimetric response, and a real-time measurement of glucose concentration. Deviations throughout the entire glucose range are detected as an inverse of the impedance in the cell due to the inverse relationship of glucose concentration and charge transfer resistance. The continuous monitoring of glucose is demonstrated by a rapid device response over two iterations of glucose concentration in ascending order: 50 μM, 400 μM, and 3.2 mM. At a sustained frequency of 10 kHz, the result shows a stable impedimetric response of 1038, 752, and 688 kΩ, respectively. The validity of the device as a continuous glucose monitoring method is carried out by repeating the cycle and observing the response.

1. Introduction: At the intersection of biological and engineering sciences lies biosensor research, a promising field that has become crucial to modern life. Defined as any device that incorporates biological, biologically derived, or biomimetic technology with a transducing element, biosensor research cascades into seemingly astronomical variations that meet the requirements of many fields including diagnostics, food safety and processing, environmental monitoring, biomedicine, and drug discovery [1]. Despite their complexities, biosensing systems are typically composed of three elements: the analyte such as food samples, human samples, environmental samples, or cell cultures; the transducer, a biological mediator; and a digital interpretation method that consisting of a signal amplifier, processor, and display interface. Biosensors are intrinsically designed to be highly selective enabling customisation of the device to a unique biological reaction by implementing specific mediators (biological elements) that have a binding affinity with the target molecule [2]. Since Clark and Lyons pioneered the first generation of glucose sensors implementing glucose oxidase enzymes to detect variations in glycemic index in 1962 [3], biodetection and monitoring have become increasingly complex.

A prominent field of study in biosensor development is the study of electrochemical behaviour in which electric signatures such as resistance, reactance, relaxation times, and diffusion effects provide valuable insight into the fluids contents and behaviour under the influence of mediated and unmediated electron transfer [4]. In biosensing relevant electrical properties that characterise biological phenomena are typically electrochemical in nature and occur in relatively close proximity to the electrode surface. As such, electrode geometry, material, and surface modification determine the sensing ability of the device. Hence, the distinct advantage of existing electrode designs that are easily incorporated into lab-on-a-chip (LOC) technologies indicates significant promise in the field of electrochemical sensing.

Impedimetric biosensors enable the observation of material properties and reactions within an electrochemical cell that can alter the systems conductivity/resistivity or capacitivity at the electrode/analyte interface. In recent years, the demand for glucose monitoring techniques is rivalled only by the expansive increase of proposed exploratory devices. As the topic matures, the research community has divided glucose sensing technology into two primary categories: sensing based on existing enzymatic technologies, and enzyme-free detection methods with the majority of emphasis placed on enzymatic sensing. Although quality improvements in enzyme-based detection are still being made, there are a number of complications associated with enzymatic glucose sensors such as difficult enzyme immobilisation procedures and environmental sensitivity [5]. Moreover, the biological nature of these devices equates to a short shelf life, high fabrication costs, and single use limitations. As the number of diabetic cases continue to rise, researchers have shifted their focus to a possible solution in non-enzymatic glucose (NEG) detection to overcome the limitations of the current technology. Referred to as the fourth generation of glucose sensors, NEG technology employs the direct interface between the electrode and target molecule without the aid of an unstable biological interface [6]. This enables the concept of real-time monitoring and long-term stability.

The new generation of glucose sensors aims to develop continuous glucose monitoring (CGM) devices replacing the current glucose sensors. Chen *et al.* [7] reviewed the current growth areas of CGM technologies and outlined current status and future perspective for CGM system. In this research, a NEG device is fabricated, characterised, and employed as a means of real-time monitoring of glucose concentration change using electrochemical impedance spectroscopy (EIS). A bare gold planar electrode in a band/gap interdigitated configuration is used. Conventional data acquisition techniques over a broad frequency range are conducted in order to obtain a fixed frequency spectrum for real-time measurement of various glucose concentrations. In addition, critical aspects of data acquisition, processing, and linearisation are also examined.

2. Design and fabrication: The electrochemical reaction between the electrode and experimental solution occurs either at the electrode surface or in close proximity. Thus, the electrodes themselves are paramount to the performance of the device. The interdigitated planar electrode (IDE) design shown in Fig. 1*a* is chosen and arranged longitudinally on the slide. Each IDE array measured 6 mm × 50 μm with a 50 μm gap between each band. Each substrate contained a total of four arrays with one (E1), three (E2), five (E3), and seven (E4) electrode pairs arranged in a band/gap configuration.

Unlike their enzymatic predecessors, NEG sensors rely on modifiers at the surface of the electrode as an electrocatalyst of glucose oxidation [8]. Numerous efforts using a vast array of porous layers

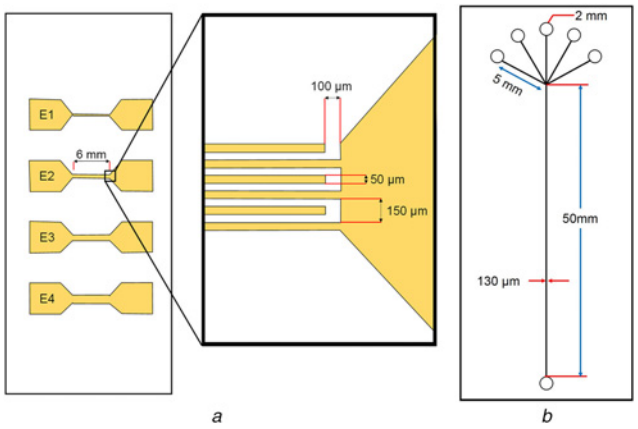

Fig. 1 *Dimensions of electrode and microfluidic channel*
a Electrode array design with band/gap dimensions. E1 has one pair, E2 has three pairs, E3 has five pairs, and E4 has seven pairs of IDEs
b Microfluidic channel design with a 100 µm × 100 µm channel width beginning with five inlets and terminating with one outlet

[9–11], graphene [12, 13], nanotubes [14], oxides [15–18], nanoparticles [19–21], and alloys [22] have been explored as potential sensing mediums in primarily amperometric and potentiometric studies. The complex nature of preparation for nanoparticles and thin film based mediators have been rigorously investigated in recent years even to the point of their necessity with numerous experiments based on data obtained from bare metal electrodes devoid of any modifiers [21]. The electrochemical kinetics and mechanisms of NEG technology remain ambiguous with limited scientific exploration. Gold is selected for the electrode due to its low oxidation potential at neutral pHs, thus limiting signal degradation due to fouling [23].

While conventional glucose screens rely on a static droplet analysis, CGM suggests a steady flow of analyte. To simulate this behaviour, the microfluidic channel shown in Fig. 1*b* is incorporated to serve as a carrier for the sample solution to each electrode interface. The microfluidic channel is designed with a 1:1 ratio of 100 µm spanning the entire length of the electrode array. Five inlets are incorporated to enable the introduction of varying analyte concentrations in rapid succession as well as a single outlet for future connections.

The integration process of electrode arrays is divided into four steps: cleaning, photolithography (Figs. 2*a* and *b*), metallisation (Fig. 2*c*), and liftoff (Fig. 2*d*). The process flow begins by cleaning a slide glass. A standard borosilicate microscope slide (Fisher Scientific 12-544-1 Pittsburgh, PA) is chosen as a substrate as it is readily available, and are easily incorporated into other LOC designs. Prior to depositing photoresist, hexamethyldisilizane is applied to the glass to improve photoresist adhesion. A 1.4 µm-thick AZ 5214E (Microchemicals GmbH, Ulm, Germany) photoresist is spun on the glass. Upon reaching ambient temperature, the slide is loaded into a UV aligner for an exposure dose of 78 mJ/cm^2.

Metal layers are deposited for electrodes on the entire substrate via electron beam evaporation. An adhesive layer, 5 nm thick of titanium, is applied followed immediately by the 100 nm functional layer of gold. Following metal deposition, the substrate is submerged in acetone for 2 min. This soaking period begins to dissolve the photoresist leaving only the metal electrode on the glass substrate. The substrate is agitated in an intermittent ultrasonic bath until no photoresist remained.

The microfluidic channel began with the fabrication of a mould master constructed in SU-8 2050 polymer photoresist on a 100 mm (100) Si wafer yielding a film of ∼130 µm (Figs. 2*e–h*). The microfluidic channel is fabricated in polydimethylsiloxane (PDMS) (Sylgard 184 Elastomer, Dow Corning, Midland, MI),

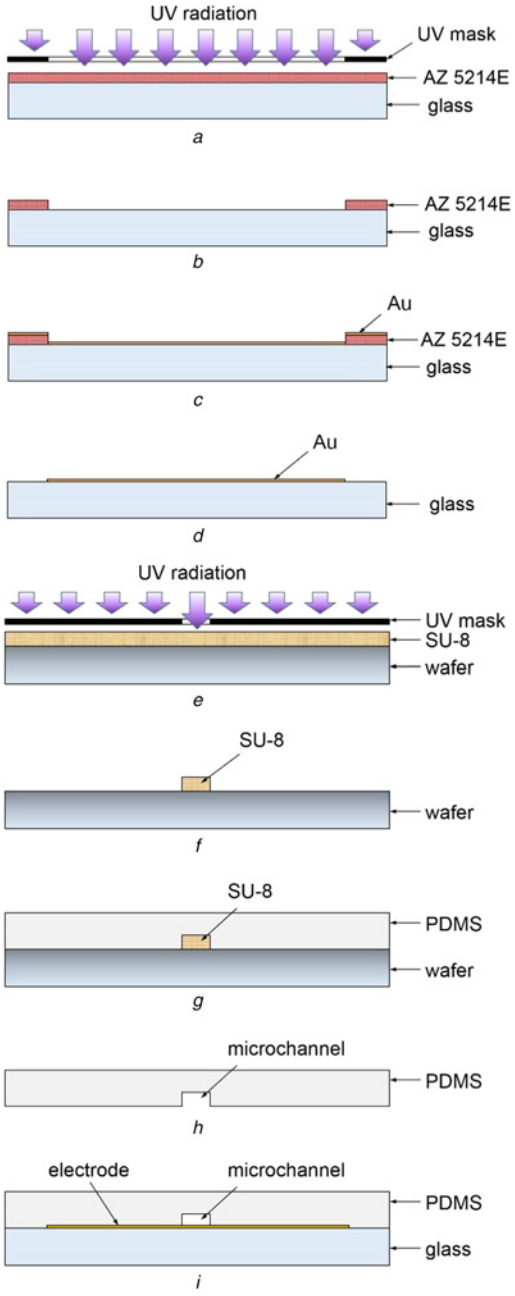

Fig. 2 *Schematic diagram of the device fabrication process*
a UV lithography
b Photoresist development
c Metal deposition
d Photoresist liftoff
e SU-8 exposure
f SU-8 development
g PDMS application over mould master
h Removal of microfluidic channel from mould master
i Bonding of PDMS microchannel with glass substrate via O_2 plasma

a 10:1 ratio of polymer resin. The cured PDMS is cut along the edges of the microfluidic structure and peeled away from the mould master resulting in the microfluidic channel. To ensure the microchannel dimensions, a sacrificial microchannel is fabricated and cleaved at different locations along the fluidic channel and measured.

The final step in device fabrication is the assembly of the PDMS microfluidic channel and the glass substrate with gold electrodes (Fig. 2*i*). An oxygen plasma bond is used to ensure a uniform permanent seal between the glass slide and the PDMS microchannel.

doi: 10.1049/mnl.2017.0894

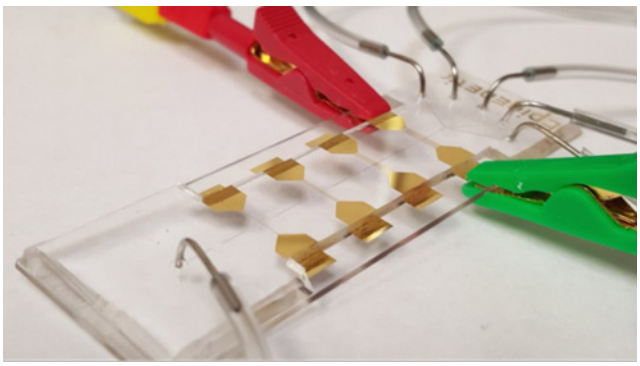

Fig. 3 *Completed device in the measurement configuration is shown with E1 positioned at the bottom and E4 connected with the potentiostat*

Upon contact, the two surfaces adhere forming a sealed device and the connecting ports are punched and connecting ports are plumbed with capillary tubing in preparation for experiments as shown in Fig. 3.

3. Experiment results: The glucose monitoring device is connected to a syringe with different glucose concentrations at the inlet and a waste reservoir at the outlet filled with deionised (DI) water to pressurise the fluidic channel and eliminate solution backflow. Each glucose solution is applied to a target electrode array and the impedance spectra are collected over the course of 90 sampling measurements from low frequency to high frequency. Each interdigitated electrode (IDE) is tested at random and the trial is repeated a total of three times using three devices.

Impedimetric devices do not require a conductive analyte solution as long as the data collection method has sufficient range to capture low- and high-level variations of resistivity/conductivity within the system. The application of an excitation voltage to an impedimetric electrochemical cell generates immediate resistive and/or capacitive responses at the electrode/analyte interface. As a result, the devices are ideal in situations where rapid detection and sensing agility are critical metrics of performance.

Four IDEs are used to establish the effects of geometric modifications of electrode surface area: E1 with a single pair of IDE, E2 with three pairs of IDE, E3 with five pairs of IDE, and E4 with seven pairs of IDE as designed in Fig. 1. Figs. 4*a–d* demonstrate the Nyquist plot for each electrode ranging from 500 Hz to 35 kHz with a 50 mV AC amplitude. A systematic decrease in cell impedance $|Z|$ is observed as the number of interdigitated pairs increase. The addition of electrode pairs increases the surface area of the electrode hence enhancing electrode and analyte interaction.

Since the interface of each electrode is limited to 100 µm × 50 µm areas, the reaction area is overwhelmed by molecules suspended in solution. While a sensing modality below 200 µM is possible in the diffusion-based portion of the impedance spectra, electrochemical diffusion is affected by a number of environmental conditions that are difficult to control such as temperature and atmospheric pressure. Hence, a fixed experimental methodology for continuous monitoring with diffusion driven reactions is difficult.

The impedimetric responses at E1, E2, and E3 are similar with regard to the mechanism of electron transfer. Dominated by diffusion, E2 and E3 are also limited in their application in continuous monitoring modes. At E4 (seven IDE pairs), the diffusion effects are greatly reduced and kinetic electron transfer begins to drive the chemical reaction at a lower frequency in comparison to E1–E3. Based on the experiment, E4 provides sufficient bonding areas to not only discriminate between glucose concentrations, but also enhance device resolution as shown in Fig. 4*d*. The increased dispersion between concentration plots indicates that interstitial glucose concentrations could be deciphered. Fig. 5

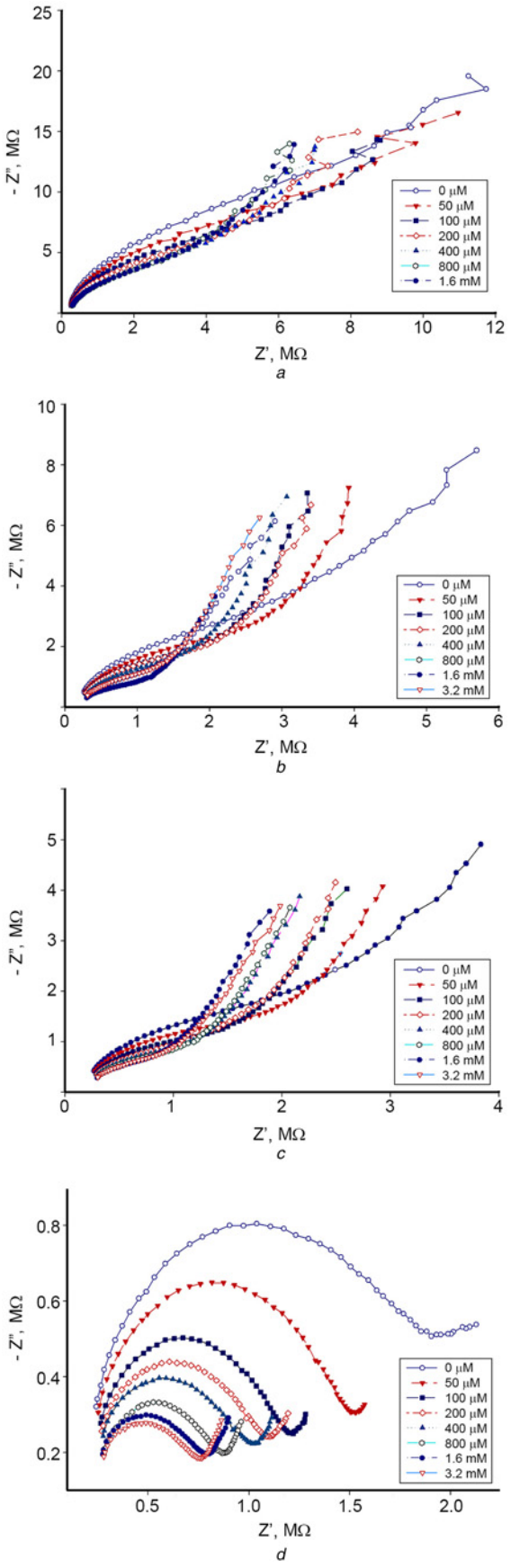

Fig. 4 *Nyquist plot for different glucose concentration from 0 M to 3.2 mM by applying frequency of 500–35 kHz for*
a E1
b E2
c E3
d E4

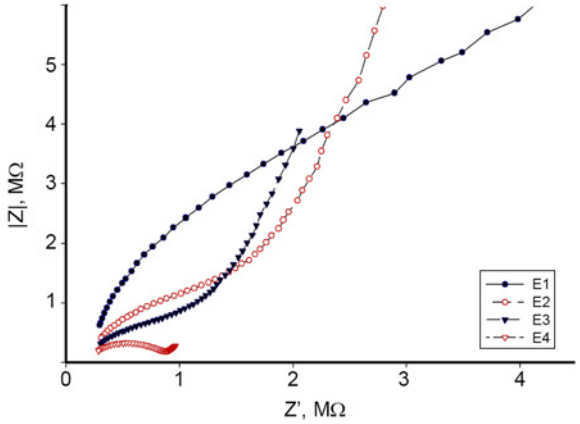

Fig. 5 *Nyquist plot with each electrode array at 800 μM concentration. As electrode surface is increased, the impedance is decreased*

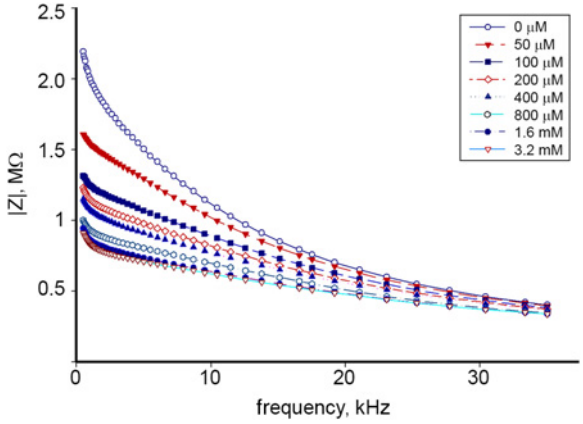

Fig. 6 *Impedance |Z| as a function of frequency at E4 for all concentrations of glucose. As frequency is increased, the dispersion between glucose concentrations decreases*

show the Nyquist plot of each electrode set at an 800 μM concentration. As the number of IDEs increases, a decrease in impedance is exhibited. The increase in physical dimensions of the electrode subsequently increases the electric field interacting with the target analyte. The target solution achieved an excitation state faster and displayed Faradic behaviour that can be readily identified and analysed. Hence, E4 is selected to conduct tests for device resolution as a function of glucose concentration as well as real-time monitoring simulations.

A measurable response to changes in glucose concentration in aqueous solution is imperative to the development of continuous monitoring efforts. The discrete significance of glucose variation on the impedance spectra at E4 under the influence of equal experimental parameters is represented in the Nyquist plot shown in Fig. 4*d*. The short linear response at low frequencies demonstrated the effects of Warburg impedance on the first time constant while the parabolic shape of each concentration characterised the effects of kinetic charge transfer.

The addition of glucose to ultrapure DI water does result in a decrease in impedance since the resistivity of water is effectively lowered by the addition of glucose [24]. This is explained by the chemical composition and interaction of both the solute and the solvent. In pure water, molecules generally do not possess sufficient free electrons to transfer current, but a process called auto-ionisation occurs continuously in water to maintain an equilibrium state. Glucose and water are polar molecules that orient themselves with respect to their opposite poles, and current flow results from the motion of electrically charged carriers in response to forces that act on them from an externally applied electric field. Under the influence of an excitation voltage, the glucose and water molecules arranged themselves with respect to the potential applied at the cathode and the current response at the anode. Ions that are free or weakly bonded are attracted to their respective opposing polarities. The increase in glucose concentration increased the number of electron carriers and additional current flow paths are formed. A decrease in overall cell impedance is observed due to the increase in charge carriers.

Variations in the impedance spectra are demonstrated when frequency is varied from 500 Hz to 35 kHz. In real-time measurement, a fixed frequency parameter is required to ensure that the various concentrations are detected by the device. Fig. 6 represents the impedance change as a function of the frequency at E4. Elevated frequencies had dramatic effects on the behaviour of the electrochemical cell that are interpreted by the Randles circuit. While charge transfer resistance and solution resistance remained unchanged, an increase in frequency resulted in an increase in the capacitive reactance demonstrated at the electrode/electrolyte interface. Furthermore, these same frequency additions marginalised the effects of Warburg impedance, and reduced the Randles cell to effectively an active solution resistance and a charge transfer resistance. Since current flows through the path of least resistance, the bulk of the resultant current signal is obtained from the lower portion of the cell.

Convergence of the data to a lower impedimetric response is a direct reflection of the increase in frequency. Due to this effect, a frequency at the lower end of the spectrum is required. While the largest dispersion is demonstrated at 1 kHz, the signal-to-noise ratio in that range is comparably lower than that of 5 and 10 kHz. Considering signal-to-noise ratio and sensor resolution, 10 kHz is chosen because of the equidistant dispersion between concentrations when compared to data obtained at 5 kHz. Fig. 7 shows the impedance values as a function of different glucose concentrations, C, measured at 10 kHz. The concentration was plotted in log scale to generate linearity curves. According to the curve fitting, the impedance is given by $|Z| = -220433 \log(C) + 43265$, and hence the sensitivity is of −220,433 Ω/decade.

CGM methods have already been established implementing a variety of enzymatic techniques. Generally, these enzyme-based mediators drive chemical reactions within the cell generating the products of the reaction to be *sensed* by the device. The inherent problems associated with enzymatic monitoring are compounded in real-time monitoring scenarios. The fixed frequency impedimetric testing method using a non-enzymatic bare gold electrode can be a viable solution. The device is connected to three different glucose solutions including 50 μM, 400 μM, and 3.2 mM and the

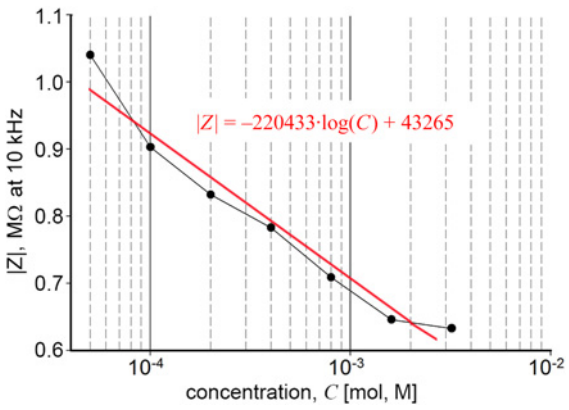

Fig. 7 *Impedance |Z| for all concentrations of glucose at 10 kHz and linear fit. |Z| = −220433 log(C) + 43265, R squared (adj.) = 0.947*

doi: 10.1049/mnl.2017.0894

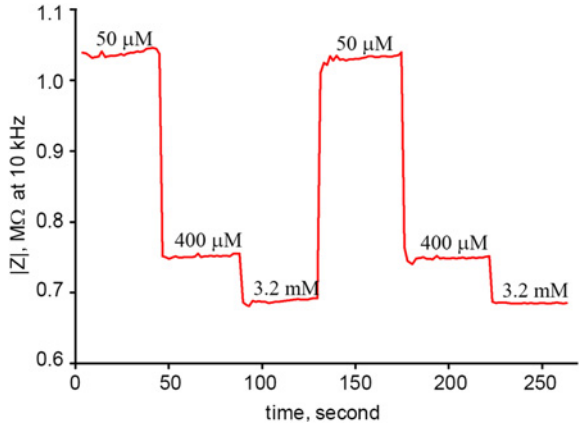

Fig. 8 *Step profile for CGM at 50 µM, 400 µM, and 3.2 mM concentrations. The cyclic nature of the profile indicates device stability throughout the duration of the test*

potentiostat and impedance analyser are programmed with the aforementioned parameters. A real-time glucose monitoring experiment is carried out in which the glucose concentration is varied over a period of 4.375 min at a sustained frequency of 10 kHz. An impedance measurement is captured every 1.75 s with concentration changes in ascending order every 45 s. The glucose concentration is cycled for two iterations to establish signal reliability. This testing methodology provided insight into the device reaction time to deviations in glucose concentration as well as simulated CGM.

A real-time glucose monitoring modality is tested with the results given in Fig. 8. A 50 µM solution is applied for the first interval of measurement generating a stable impedimetric response of 1038 ± 4 kΩ that remains constant until the 400 µM solution is introduced into the channel. The increase in glucose concentration enables a rapid decrease in impedance to 752 ± 1.9 kΩ where the signal remained until the final 3.2 mM solution is applied. In this case, the impedimetric response reduces to 688 ± 2.8 kΩ. The validity of the device as a CGM method is tested by repeating the cycle and observing the response. The impedance values for the second measurement iteration are 1031 ± 3.4, 750 ± 2.2, and 685 ± 0.4 kΩ, respectively.

To establish a real-time monitoring technique, three critical metrics are considered: device sensitivity, response time, and reliability. Impedance data captured in real time demonstrates both sensing efficacy and device response to glucose variation. Although the impedance shift is reduced in magnitude, increases in concentration induce a rapid impedimetric decrease. Deviations in magnitude are contributed to the glucose solution approaching saturation as concentration increased. The addition of glucose to water facilitates current flow through the solution from the working electrode to the reference electrode.

4. Conclusion: The research conducted reveals that EIS measurement coupled with a non-enzymatic gold electrode is an effective means of detecting variation in glucose concentration in aqueous solution. Iterative analysis of impedimetric responses to electrode surface area, excitation frequency, and glucose concentration were investigated to establish a CGM method. It was shown that as glucose concentration increased, cell impedance decreased. Furthermore, the results suggest that device resolution increased as electrode surface area increased. Primary function of the device relied on the ability to sense variation in glucose concentration. Repeated tests indicated that the addition of glucose molecules reduced impedance values by enriching the solution with ions that served as charge carries.

Non-enzymatic CGM device is able to respond to changes in the solution. A distinct advantage of EIS is the ability to measure in the time domain allowing the calculation of discrete response time measurements. The sampling interval in this experiment is fixed for 150 measurements at 1.75 s intervals. The device is capable of detecting variations in glucose at a rate less than the measurement interval. The rapid response is attributed to the absence of a mediation layer which enabled the excitation of charge carriers and consequently rapid detection of concentration variations.

5 References

[1] Lafleur J.P., Jonsson A., Senkbeil S., *ET AL.*: 'Recent advances in lab-on-a-chip for biosensing applications', *Biosens. Bioelectron.*, 2016, **76**, pp. 213–233

[2] Chaubey A., Malhotra B.D.: 'Mediated biosensors', *Biosens. Bioelectron.*, 2002, **17**, pp. 441–456

[3] Clark L.C.J., Lyons C.: 'Electrode systems for continuous monitoring in cardiovascular surgery', *Ann. New York Acad. Sci.*, 1962, **102**, pp. 29–45

[4] Shervedani R.K., Mehrjardi A.H., Zamiri N.: 'A novel method for glucose determination based on electrochemical impedance spectroscopy using glucose oxidase self-assembled biosensor', *Bioelectrochemistry*, 2006, **69**, (2), pp. 201–208

[5] Park S., Boo H., Chung T.D.: 'Electrochemical non-enzymatic glucose sensors', *Anal. Chim. Acta*, 2006, **556**, (1), pp. 46–57

[6] Lee S.J., Yoon H.S., Xuan X., *ET AL.*: 'A patch type non-enzymatic biosensor based on 3d sus micro-needle electrode array for minimally invasive continuous glucose monitoring', *Sens. Actuators B, Chem.*, 2016, **222**, pp. 1144–1151

[7] Chen C., Zhao X.L., Li Z.H., *ET AL.*: 'Current and emerging technology for continuous glucose monitoring', *Sensors (Basel)*, 2017, **17**, p. 182

[8] Pletcher D.: 'Electrocatalysis: present and future', *J. Appl. Electrochem.*, 1984, **14**, pp. 403–415

[9] Dong W., Luo J., He H., *ET AL.*: 'A reinforced composite structure composed of polydiacetylene assemblies deposited on polystyrene microspheres and its application to H5n1 virus detection', *Int. J. Nanomed.*, 2013, **8**, pp. 221–232

[10] Lee Y.-J., Park D.-J., Park J.-Y., *ET AL.*: 'Fabrication and optimization of a nanoporous platinum electrode and a non-enzymatic glucose micro-sensor on silicon', *Sensors*, 2008, **8**, pp. 6154–6164

[11] Li Y., Song Y.-Y., Yang C., *ET AL.*: 'Hydrogen bubble dynamic template synthesis of porous gold for nonenzymatic electrochemical detection of glucose', *Electrochem. Commun.*, 2007, **9**, (5), pp. 981–988

[12] El-Ads E.H., Galal A., Atta N.F.: 'Electrochemistry of glucose at gold nanoparticles modified graphite/Srpdo3 electrode – towards a novel non-enzymatic glucose sensor', *J. Electroanal. Chem.*, 2015, **749**, pp. 42–52

[13] Yazid S.N., Isa I.M., Hashim N.: 'Novel alkaline-reduced cuprous oxide/graphene nanocomposites for non-enzymatic amperometric glucose sensor application', *Mater. Sci. Eng. C*, 2016, **68**, pp. 465–473

[14] Cai Z.-X., Liu C.-C., Wu G.-H., *ET AL.*: 'Palladium nanoparticles deposit on multi-walled carbon nanotubes and their catalytic applications for electrooxidation of ethanol and glucose', *Electrochim. Acta*, 2013, **112**, pp. 756–762

[15] Ghanbari K., Babaei Z.: 'Fabrication and characterization of non-enzymatic glucose sensor based on ternary Nio/Cuo/polyaniline nanocomposite', *Anal. Biochem.*, 2016, **498**, pp. 37–46

[16] Rahman M.M., Ahammad A.J., Jin J.H., *ET AL.*: 'A comprehensive review of glucose biosensors based on nanostructured metal-oxides', *Sensors (Basel)*, 2010, **10**, (5), pp. 4855–4886

[17] Yang H., Zhu Y.: 'Size dependence of Sio2 particles enhanced glucose biosensor', *Talanta*, 2006, **68**, (3), pp. 569–574

[18] Zhong Y., Shi T., Liu Z., *ET AL.*: 'Ultrasensitive non-enzymatic glucose sensors based on different copper oxide nanostructures by in-situ growth', *Sens. Actuators B, Chem.*, 2016, **236**, pp. 326–333

[19] Chung J., Kang J.S., Jurng J.S., *ET AL.*: 'Fast and continuous microorganism detection using aptamer-conjugated fluorescent nanoparticles on an optofluidic platform', *Biosens. Bioelectron.*, 2015, **67**, pp. 303–308

[20] Ensafi A.A., Zandi-Atashbar N., Rezaei B., *ET AL.*: 'Silver nanoparticles decorated carboxylate functionalized Sio2, new nanocomposites for non-enzymatic detection of glucose and hydrogen peroxide', *Electrochim. Acta*, 2016, **214**, pp. 208–216
[21] Soomro R.A., Akyuz O.P., Ozturk R., *ET AL.*: 'Highly sensitive non-enzymatic glucose sensing using gold nanocages as efficient electrode material', *Sens. Actuators B, Chem.*, 2016, **233**, pp. 230–236
[22] Li H., Guo C.Y., Xu C.L.: 'A highly sensitive non-enzymatic glucose sensor based on bimetallic Cu-Ag superstructures', *Biosens. Bioelectron.*, 2015, **63**, pp. 339–346
[23] Pasta M., La Mantia F., Cui Y.: 'Mechanism of glucose electrochemical oxidation on gold surface', *Electrochim. Acta*, 2010, **55**, (20), pp. 5561–5568
[24] Yoon G.: 'Dielectric properties of glucose in bulk aqueous solutions: influence of electrode polarization and modeling', *Biosens. Bioelectron.*, 2011, **26**, pp. 2347–2353

doi: 10.1049/mnl.2017.0894